

Purification and Properties of Human Blue-Light Photoreceptor Cryptochrome 2[†]

Sezgin Özgür and Aziz Sancar*

Department of Biochemistry and Biophysics, University of North Carolina School of Medicine,
Chapel Hill, North Carolina 27599

Received October 7, 2002; Revised Manuscript Received January 23, 2003

ABSTRACT: Cryptochromes are blue-light photoreceptors that regulate the circadian clock in animals and growth and development in plants. Cryptochromes have high sequence homology to DNA photolyase but appear to lack photorepair activity. All previous work on cryptochromes was performed with protein expressed in heterologous systems; hence, biochemical and photochemical studies performed with these proteins were subject to certain limitations. In this study, we purified cryptochrome 2 (hCRY2) from human cells and characterized it. We find that hCRY2 exhibits fluorescence properties consistent with the presence of folate and flavin cofactors. Cryptochrome 2 binds to double-stranded DNA weakly and to single-stranded DNA with higher affinity, and this binding is further stimulated by the presence of a (6-4) photoproduct. However, light has no effect on the cryptochrome 2-(6-4) photoproduct complex. These findings reveal new properties of this protein already known to function as a circadian photoreceptor and a light-independent negative transcriptional regulator of the clock genes.

Cryptochromes are blue-light photoreceptors that regulate the circadian clock in animals and growth and development in plants (1–3). There have been extensive genetic studies on the function of cryptochromes both in plants (2, 4) and in animals (1, 3, 5) that have revealed their roles in growth and development in *Arabidopsis*, circadian photoreception in the mouse, *Drosophila*, and *Arabidopsis* and a central role in the molecular clockwork of animals. However, the biochemical basis of these various effects is not known, in part because of the lack of an in vitro assay and in part to the lack of cryptochromes purified from their natural sources.

Cryptochromes have high degrees of sequence identity to DNA photolyases that are known to contain FAD¹ and folate (or in rare cases, 5-deazariboflavin instead of folate) as chromophore/cofactors (6–8). Indeed, both *Arabidopsis* (9, 10) and human (11) cryptochromes expressed in *Escherichia coli* or in insect cells (12) contain FAD and a pterin. However, these cofactors are present at significantly substoichiometric levels in recombinant proteins overproduced in heterologous systems. Moreover, cryptochromes purified from heterologous expression systems tend to aggregate, and the combination of these two factors, substoichiometric cofactor content and poor solubility, has prevented biochemical and photochemical characterization of cryptochromes. Our attempts to purify animal cryptochromes from native sources using mouse, rat, and cow retinas and bovine testis

where cryptochromes 1 and 2 are relatively abundant (13, 14) were unsuccessful mainly because of lack of a biochemical assay for cryptochrome. To overcome these problems, we constructed HeLa cell lines expressing tagged human CRY1 and CRY2 proteins. Here, we describe the purification and properties of the hCRY2 protein. Spectroscopic analysis indicates that hCRY2 contains both flavin and folate. The purified protein binds to DNA and with higher affinity to DNA containing a (6-4) photoproduct, but it does not repair the photodamage.

MATERIALS AND METHODS

Molecular Modeling. The crystal structures of DNA photolyases from *E. coli* (15) and *A. nidulans* (16) were used as structural templates for homology modeling using the Modeler module of Insight II molecular modeling system from Accelrys Inc. (www.accelrys.com). The C-terminal 106 amino acids of hCRY2 (total length 593 amino acids) that constitutes a separate domain with no homology to photolyases (7, 11) was not included in the modeling operation. The modeled hCRY2 figure was created with SPOCK.

Derivation of a HeLa Cell Line Expressing Tagged hCRY2. The hCRY2 gene was amplified by PCR using pUNC1996-2 plasmid (11) as template, and the PCR product was cloned into pcDNA4/Myc-His (Invitrogen). Then, an oligomer encoding the Flag epitope was cloned in-frame into the 3' terminus of the hCRY2 to obtain pSÖ2002, which expresses hCRY2 with Myc, His, and Flag tags at the carboxy terminus. The sequence of the gene in this construct was confirmed by DNA sequencing of the entire hCRY2 insert.

HeLa cells grown in alpha-MEM (Gibco/BRL) supplemented with 10% fetal bovine serum were transfected with pSÖ2002 using Lipofectin (Invitrogen) according to the manufacturer's procedure. Transfected cells were selected

[†] This work was supported by the NIH Grant GM31082.

* Corresponding author. Phone: (919) 962-0115. Fax: (919) 843-8627. E-mail: Aziz_Sancar@med.unc.edu.

¹ Abbreviations: hCRY1, human cryptochrome 1; hCRY2, human cryptochrome 2; FAD, flavin adenine dinucleotide; HEPES, *N*-(2-hydroxyethyl) piperazine-*N'*-2-propanesulfonic acid; Tris-HCl, tris-(hydroxymethyl) aminoethane; DTT, dithiothreitol; EDTA, ethylenediamine tetraacetic acid; SDS-PAGE, sodium dodecyl sulfate-polyacrylamide gel electrophoresis; BSA, bovine serum albumin; TBE, Tris-borate/EDTA electrophoresis buffer; ssDNA, single-strand DNA; dsDNA, double-strand DNA; Per1, Period 1; Per2, Period 2.

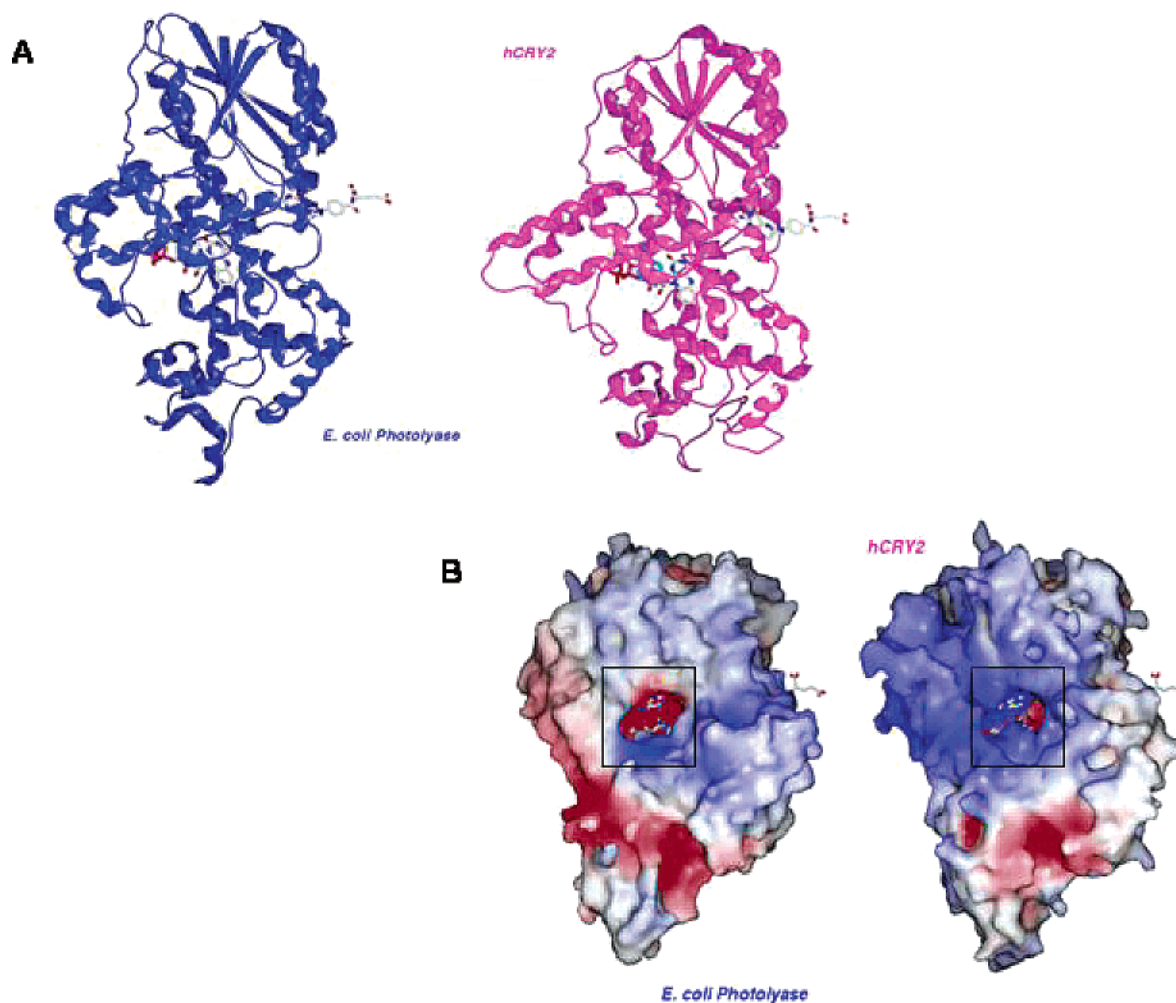


FIGURE 1: Computer-generated 3-D structure of hCRY2. The model was generated by the Insight II molecular modeling system using the experimentally determined structures of the *E. coli* and *A. nidulans* photolyases as templates and excluding the C-terminal 106 amino acids of hCRY2. The figure shows (A) ribbon diagram and (B) surface potential representations of the *E. coli* photolyase structure and the hCRY2 model. In the surface potential representation, the color scheme is as follows: blue, positive charge; red, negative charge; and white, neutral.

by resistance to Zeocin (Invitrogen) and subcloned for several rounds to isolate eight independent transfectants expressing the tagged hCRY2 at different levels as determined by immunoblotting. Aliquots of the cell lines were stored in liquid nitrogen.

Purification of hCRY2 from HeLa Cells. The HeLa/hCRY2-Flag stably transfected cell line was grown in suspension in batches of 10 L. The cells were collected by spinning at 1500g for 10 min, and the packed cells were stored at -80°C . The whole cell-free extract was prepared from the frozen cells as described previously (11) and dialyzed into buffer A, which contains 25 mM Hepes-KOH, pH 7.9, 100 mM KCl, 12 mM MgCl_2 , 0.5 mM EDTA, and 17% (v/v) glycerol. Cell-free extract (750 mg total protein) from the 10 L culture was incubated with 0.5 mL of anti-FLAG M2 affinity resin (Sigma) in Buffer A overnight at 4°C . The beads were washed with 5 mL of Buffer B (20 mM Tris-HCl, pH 7.4) containing 1 M NaCl and then with 5 mL of Buffer B containing 150 mM NaCl twice. The bound protein was eluted with 3 mL of Buffer C, which contained 50 mM Tris-HCl, pH 7.4, 150 mM NaCl, 10% glycerol, and 100 $\mu\text{g}/\text{mL}$ Flag peptide (Sigma). The purified protein was dialyzed against Buffer D (50 mM Tris-HCl, pH 7.4, 100 mM KCl, 1 mM EDTA, and 50% glycerol) and stored at

-20°C . Typical yield was 5–15 μg of hCRY2 from 10 L of HeLa cells. Because of limited amounts of hCRY2 that were available, it was not possible to determine the stoichiometry of the cofactors by absorption spectroscopy. However, we could estimate $>30\%$ saturation for both flavin and folate by fluorescence spectroscopy. The (6-4) photolyase of *Drosophila melanogaster*, which was used in some of the control experiments, was purified as described previously (17).

The quality of the purified hCRY2 was analyzed with both silver staining and immunoblotting of SDS-PAGE gels using standard procedures. In the immunoblot, hCRY2 was probed with the anti-Myc antibody (Invitrogen), and the antigen-antibody complex was detected by the alkaline phosphatase method (Promega).

DNA Binding Assay. Electrophoretic mobility shift assay was used to investigate the interaction of hCRY2 with DNA. For nonspecific binding, a 5'-labeled random sequence synthetic oligomer alone or after annealing to a complementary oligomer was used to measure binding to single- or double-stranded DNA, respectively. hCRY2 at indicated concentrations was incubated with 0.1 nM DNA in a 20 μL reaction containing 17.5 mM Tris-HCl, pH 7.4, 52.5 mM NaCl, 0.35 mM EDTA, 5 mM DTT, 0.1 $\mu\text{g}/\mu\text{L}$ BSA, and

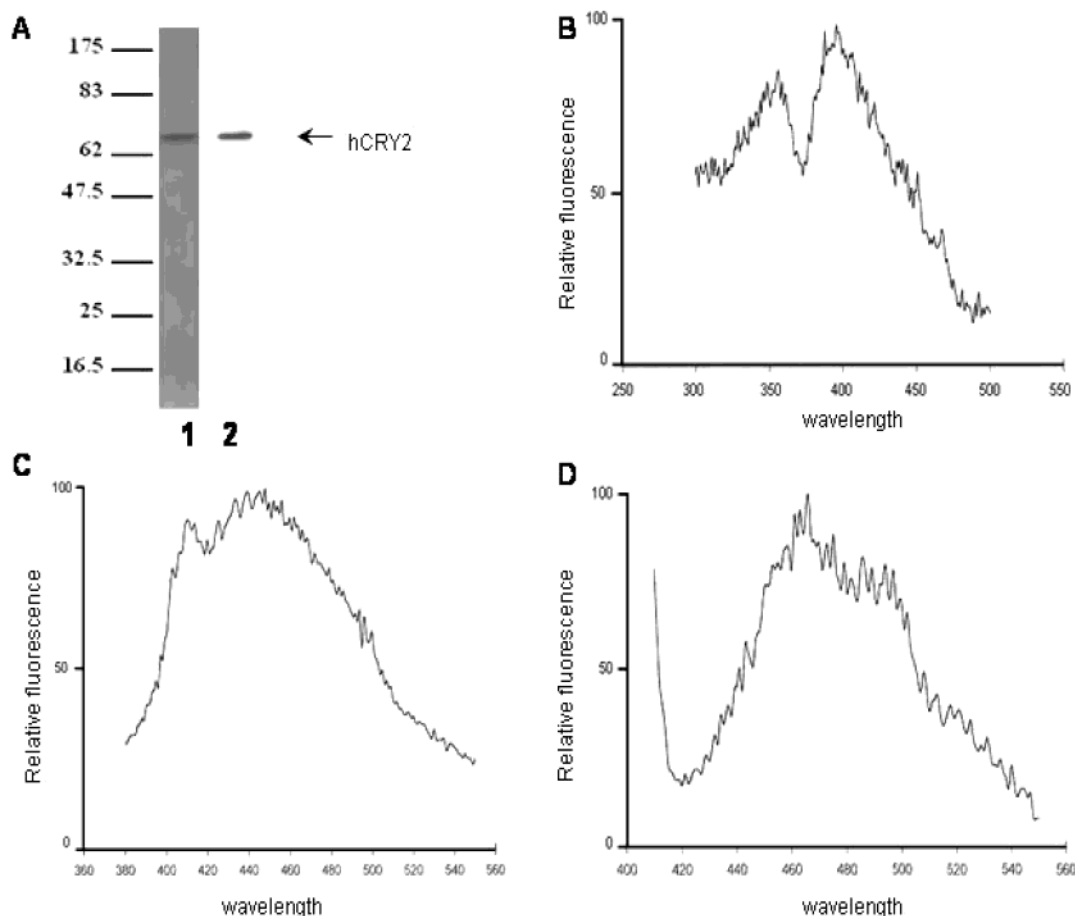


FIGURE 2: Purification and spectroscopic properties of hCRY2. (A) Purified hCRY2 analyzed on SDS-PAGE by silver staining (lane 1) or immunostaining (lane 2). Both lanes contained approximately 100 ng of protein. (B) Fluorescence excitation spectrum with λ emission at 520 nm. The excitation spectrum is consistent with a flavin fluorophore. (C) Fluorescence emission spectrum with $\lambda = 360$ nm excitation. The spectrum is consistent with the emission spectrum of hCRY2-associated methenyltetrahydrofolate. (D) Fluorescence emission spectrum with $\lambda = 400$ nm excitation. The 460 nm peak and the 505 nm shoulder are consistent with the presence of MTHF (460 nm) and FAD (505 nm) in hCRY2. These are uncorrected fluorescence spectra.

17.5% (v/v) glycerol for 20 min at 25 °C. The complexes were separated on 5% nondenaturing polyacrylamide gel in 0.5 X TBE (25 mM Tris-borate, pH 7.9, 0.6 mM EDTA). Electrophoresis was carried out at 4 °C for 1.5–2 h. For binding to (6-4) photoproduct, a 46-mer with a centrally located (6-4) photoproduct with internal label at the 5th phosphodiester bond 5' to the lesion was prepared as described previously (17). The DNA binding assays were performed as described elsewhere (18) with minor modifications. Briefly, 0.1 nM DNA was incubated with the indicated concentrations of hCRY2 for 20 min at 25 °C in binding buffer containing 17.5 mM Tris-HCl, pH 7.4, 52.5 mM NaCl, 0.35 mM EDTA, 5 mM DTT, 0.1 μ g/ μ L BSA, and 2.5% (v/v) glycerol. For antibody supershift assay, hCRY2 was preincubated with Anti-Myc antibodies (Invitrogen) for 30 min on ice in the presence of 0.4 mM DTT. The DNA-protein complexes were visualized by autoradiography. Quantitative analysis of binding was performed by scanning on a model 860 Storm PhosphorImager (Molecular Dynamics) and analyzed with ImageQuant software (version 5.0, Molecular Dynamics).

Photoreactivation Assay. The photoreactivation assay with the (6-4) photoproduct was conducted as described previously (17) using a 46-mer single-stranded oligomer containing a T-T (6-4) photoproduct in the center.

RESULTS

Structure of hCRY2. Currently, the crystal structure of a cryptochrome is not available. However, the sequence of mammalian cryptochromes 1 and 2 reveal a striking sequence homology to DNA photolyase not only in amino acids involved in FAD binding but also in amino acids that have been implicated in DNA binding (7, 8). Using the crystal structure of photolyase as a template, we wished to generate a model of hCRY2 to find out if the structural features of photolyase (namely, a positively charged strip running the length of the enzyme and a hole in the middle of this strip that leads to the FAD cofactor in the core of the protein) implicated in DNA binding (15) are conserved in cryptochrome. Using the *E. coli* (15) and the *A. nidulans* (16) photolyases as structural templates and the Modeler module of Insight II molecular modeling system from Accelrys, we built a model of hCRY2 that is shown in Figure 1. The theoretical model of hCRY2 is a valid structure overall. The Profiles-3-D/verify self-compatibility scores indicate that the final theoretical structure for hCRY2 was nearly as compatible with the hCRY2 sequence as the experimentally determined *A. nidulans* photolyase with its sequence. Considering the high degree of sequence homology between

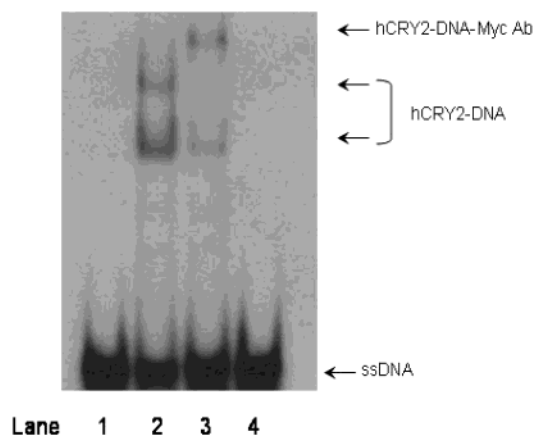


FIGURE 3: Binding of hCRY2 to DNA. hCRY2 (7 nM) was incubated with 0.1 nM of a 5'-labeled 65-nt long single-stranded DNA, and then the complexes were separated on 5% nondenaturing polyacrylamide gel and autoradiographed. Lane 1, DNA alone; lane 2, DNA plus hCRY2; lane 3, DNA plus hCRY2 plus anti-Myc antibody, which binds to the Myc tag on hCRY2; lane 4, DNA plus anti-Myc antibody.

cryptochromes and photolyases, the overall structural similarity was expected. However, the conservation of the DNA binding groove and the cyclobutane dimer cavity (15) in cryptochrome was surprising because hCRY2 is not known to possess any biological activity that involves DNA binding (1, 20–22). To find out whether hCRY2, in addition to its

other functions, has a DNA binding activity, we performed electrophoretic mobility shift assays with hCRY2 purified from human cells to near homogeneity.

Purification of hCRY2 from Human Cells. Attempts to carry out DNA binding by gel retardation with hCRY2 expressed in *E. coli* or insect cells were compounded by protein aggregation and trapping of DNA in the origin of the polyacrylamide gel. Moreover, the vast majority of the hCRY2 expressed in these heterologous systems lacks cofactors and hence is not amenable to photochemical analysis. Thus, we decided to use hCRY2 purified from its native host. We constructed a mammalian expression vector expressing hCRY2 fused to peptide tags for affinity purification, transfected HeLa cells with this construct, and isolated several cell lines expressing hCRY2. The level of expression varied by a factor of 10 among the various isolates. We chose one of the cell lines, HeLa/hCRY2-1, expressing moderate level of hCRY2 for protein purification to optimize for protein yield and cofactor incorporation.

Several micrograms of hCRY2 were purified to apparent homogeneity by immunochromatography on FLAG M2 affinity resin (Sigma). The purified protein revealed a single band of the expected molecular weight as analyzed by SDS-PAGE followed by silver staining or immunoblotting with anti-hCRY2 antibodies (Figure 2A). Importantly, fluorescence spectroscopy indicated that the purified protein contained both the flavin and the folate cofactors. When

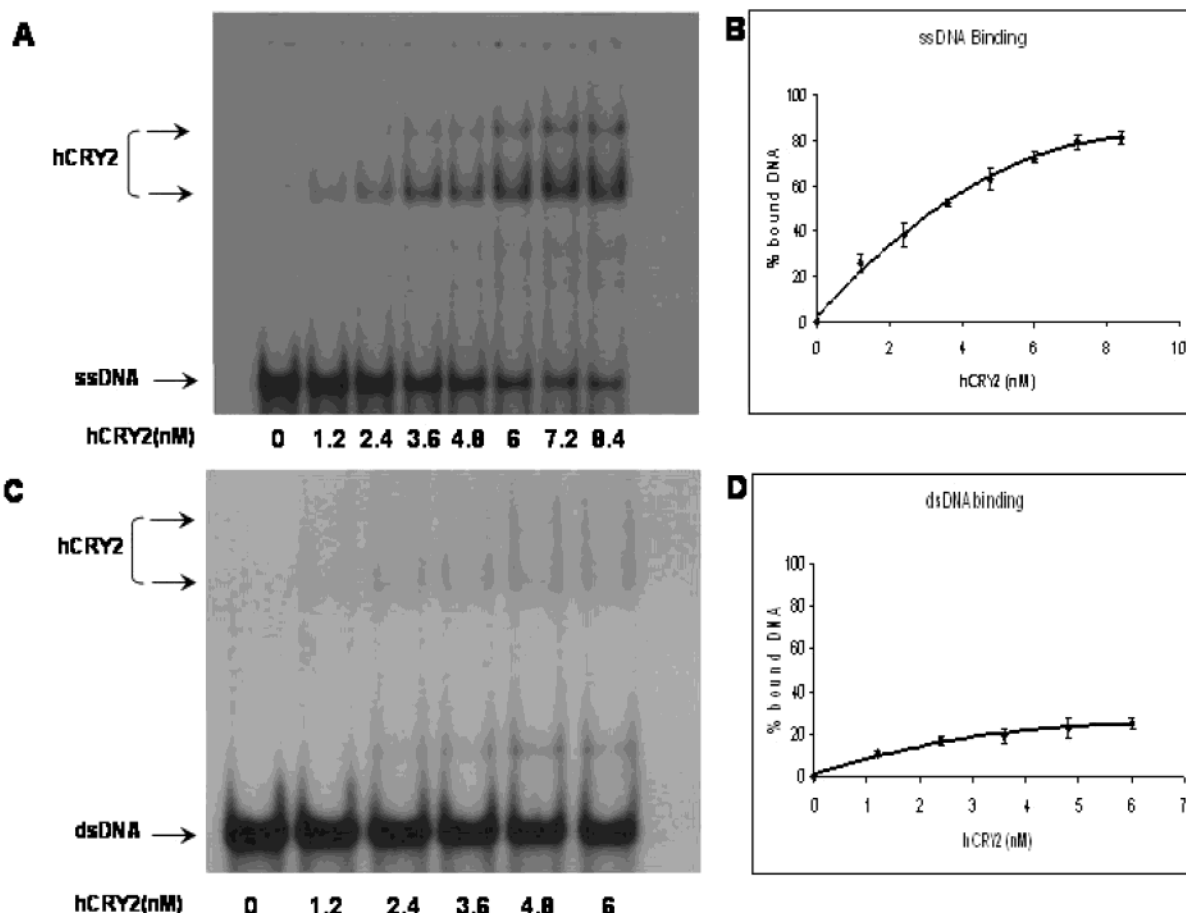


FIGURE 4: Binding of hCRY2 to single- and double-stranded DNAs. The hCRY2 at the indicated concentrations was incubated with 0.1 nM 65-nt long (A) ssDNA or (B) duplex of the same length, and the protein–DNA complexes were separated on 5% nondenaturing polyacrylamide gel and subjected to autoradiography. Left panels show representative autoradiogram, and the right panels show quantitative analysis of data from three independent experiments. The bars indicate standard errors.

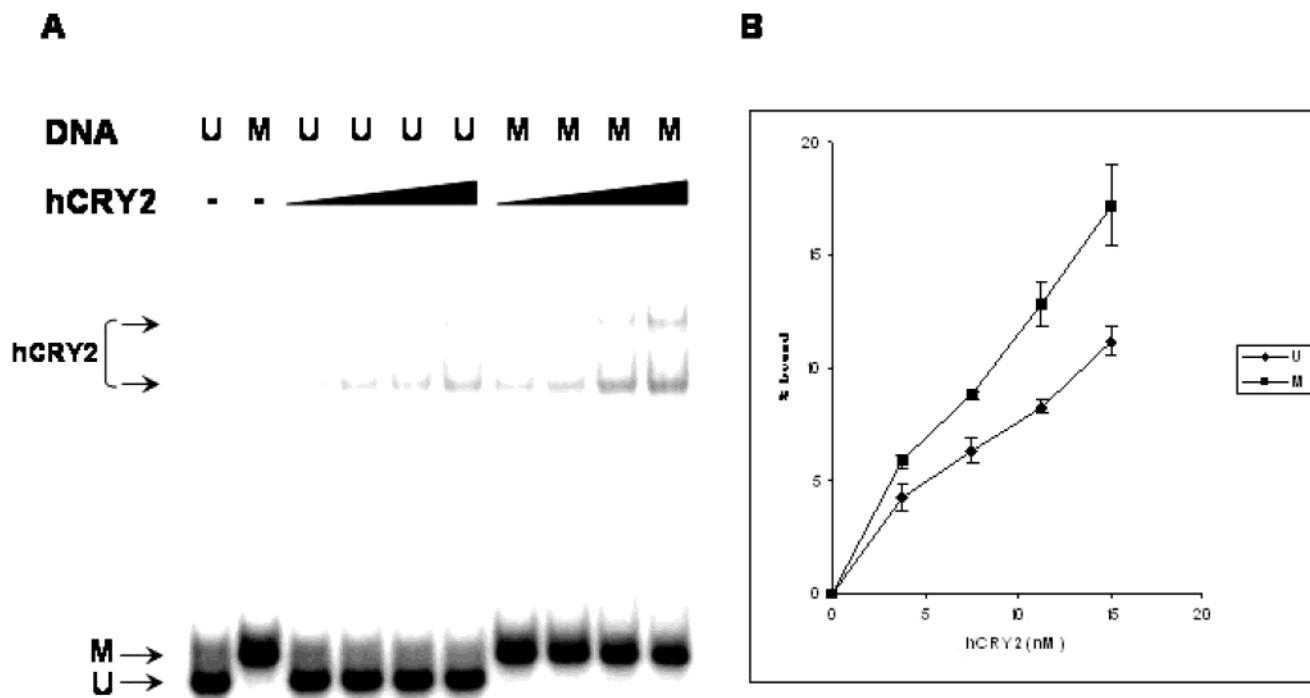


FIGURE 5: Preferential binding of hCRY2 to (6-4) photoproduct containing DNA. A 46-nucleotide-long ssDNA without (U) or with (M) a (6-4) photoproduct was incubated with increasing concentrations of hCRY2, and the DNA–protein complexes were visualized by the band shift assay. Left panel, autoradiograph of a representative gel; right panel, quantitative analysis of three binding experiments including the one shown on the left. Bars indicate standard error. Note that the affinity of hCRY2 to DNA increases with increasing DNA length and hence the lower affinity in this figure relative to that in Figure 4.

emission was monitored at 520 nm, the excitation spectrum revealed maxima at 370 and 430 nm, characteristic of flavin (Figure 2B). Similarly, excitation at 360 nm produced an emission spectrum with a 440–460 nm maximum (Figure 2C) consistent with the presence of methenyltetrahydrofolate (23). Finally, excitation at 400 nm resulted in an emission spectrum with a maximum at 460–470 nm and a shoulder at 505 nm (Figure 2D), consistent with the combined pterin and flavin fluorescence spectra as has been observed in folate class photolyases (24, 25).

DNA Binding of hCRY2. The strong structural similarity of hCRY2 to photolyase suggested that cryptochrome may also bind DNA. We tested for DNA binding by electrophoretic mobility shift-assay. Figure 3 shows that hCRY2 binds DNA (lane 2) and that this binding is not due to a contaminant in the hCRY2 preparation because the DNA–protein complex is supershifted with antibodies to the hCRY2 tag (lane 3). Pilot experiments indicated that cryptochromes may have higher affinity to single-stranded DNA than double-stranded duplex. Therefore, we performed protein titration curves with both types of DNAs. Figure 4A,B shows that hCRY2 binds to ssDNA with relatively high affinity ($K_D \sim 5 \times 10^{-9}$ M for the oligomer). In contrast, the affinity to dsDNA is much lower (Figure 4C,D), and with our experimental system we were unable to obtain sufficient binding to calculate a K_D for dsDNA. With the available data, a K_D of 10^{-7} M or higher is estimated. This is in contrast with DNA photolyase, which binds to single- and double-stranded DNAs with comparable affinities (6).

Effect of Damage on DNA Binding. Having found that hCRY2 binds DNA we wished to find out whether, like photolyase, it has higher affinity to damaged DNA. Since

cryptochromes have higher sequence homology to (6-4) photolyases than cyclobutane pyrimidine dimer photolyases (7, 26), we used single-stranded DNA containing a (6-4) photoproduct as a probe. The results shown in Figure 5 indicate that hCRY2 does indeed bind to damaged DNA with higher affinity. Thus, it appears that cryptochrome has maintained some of the photolyase structural features that confer damage specific binding. Previously, we have reported that human cell extract containing cryptochromes lacked photolyase activity and concluded that cryptochromes do not repair DNA (11). However, it was conceivable that the amount of cryptochrome in cell extract was insufficient to yield repair signal that could be detected by the specific assay we used. Hence, we tested hCRY2 in the present experimental system under conditions of specific binding to the (6-4) photoproduct-containing oligomer. The results are shown in Figure 6. The control (6-4) photolyase binds to damaged DNA with high specificity and upon photoreactivation repairs the lesion and dissociates from DNA (Figure 6A,B). In contrast, the binding of hCRY2 to the (6-4) photoproduct containing oligomer is not affected by light (Figure 6C,D). Thus, we conclude that cryptochrome binds to DNA and in particular to ssDNA with moderately high affinity and to DNA containing (6-4) photoproducts with higher affinity but that it has no DNA repair activity.

DISCUSSION

Despite intensive studies for about a decade, the photochemical reaction performed by cryptochromes is still not known. It is known that cryptochromes are required for blue-light inhibition of hypocotyl elongation in *Arabidopsis* (27, 28) for light-induced Tim protein degradation in *Drosophila*

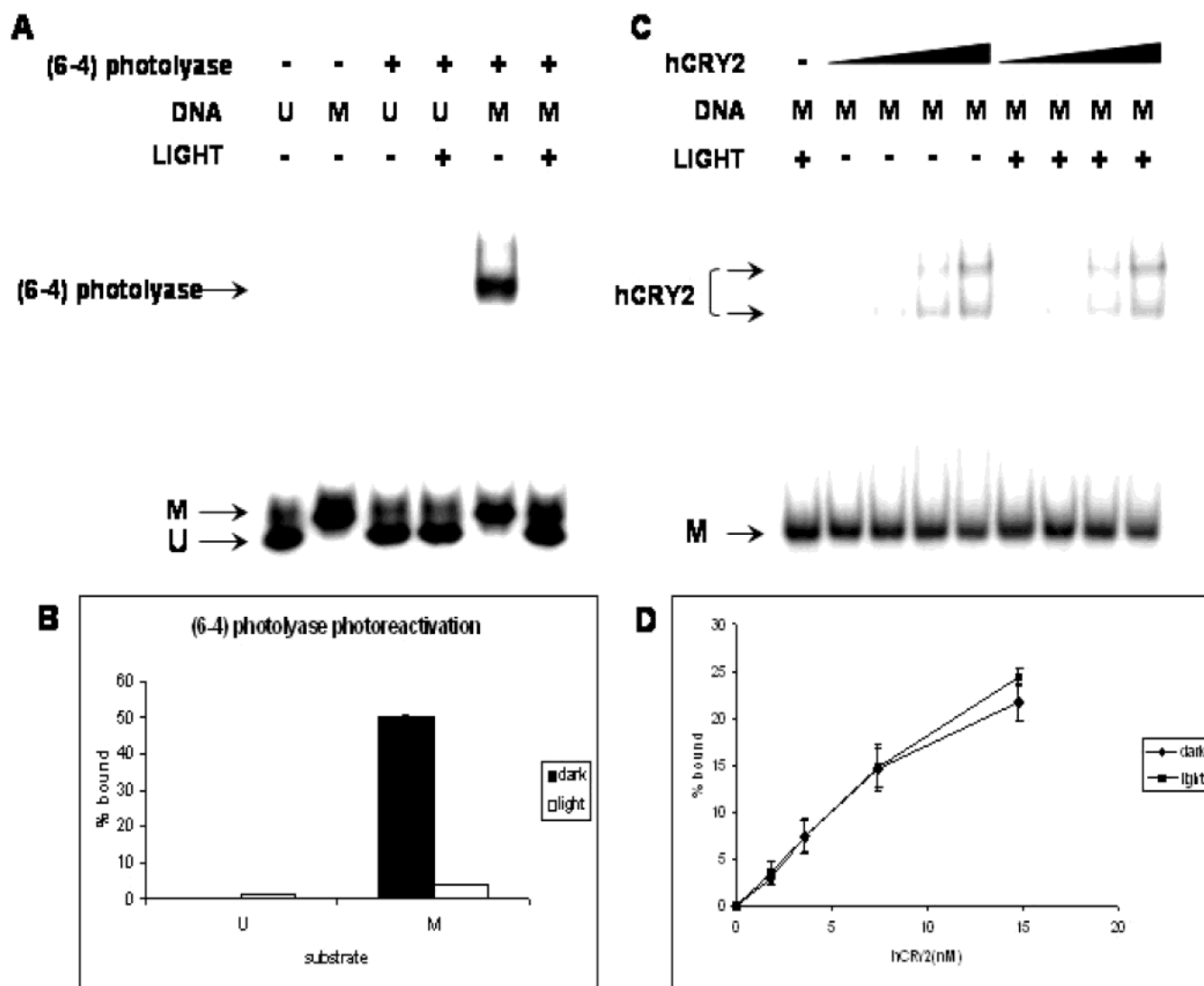


FIGURE 6: hCRY2 does not repair (6-4) photoproduct. The left panels show control experiments with (6-4) photolyase incubated with unmodified (U) or modified (M) 46-nt DNA with and without photoreactivation as indicated. The top panel is a mobility shift assay, and the bottom panel is a quantitative analysis of the binding data. The right panels show binding of hCRY2 to (6-4) photoproduct containing a 46-mer oligomer and separated on polyacrylamide gel without and with exposure to light. Top panel shows binding data with increasing concentrations of hCRY2, and the bottom panel shows quantitative analysis of three experiments including the one shown in the top panels. Bars indicate standard deviation.

(29) and for optimal photic induction of immediate early genes in the suprachiasmatic nuclei (SCN) and for the pupillary light responses of the mouse (20, 30–32). Furthermore, certain blue-light specific effects on cryptochromes have been observed in vivo. The *Arabidopsis* CRY2 is phosphorylated and degraded upon exposure of the plant to blue-light (28, 33). Similarly, in *Drosophila* CRY and its interacting partner Tim are degraded upon exposures of the flies to light (29), and in the yeast two-hybrid assay light promotes Cry–Tim protein–protein interaction (22, 34). The most parsimonious explanation for all these phenomena is that cryptochrome is a phylogenetically widespread blue-light photoreceptor. However, all (or nearly all) these data are also consistent with cryptochrome being an essential component of the phototransduction pathway rather than being a photoreceptor itself. Clearly, a photochemical cycle initiated by cryptochrome must be demonstrated to formally prove that cryptochrome is a photoreceptor. Efforts toward this goal have been frustrated because of lack of purified

native cryptochrome and difficulties in identifying a cryptochrome substrate.

Cryptochrome, like photolyase, in addition to its light function also performs a dark function (1, 20), and in contrast to paucity of information on its light function there are a considerable amount of data on its dark function. Lack of cryptochrome in mice results in increased transcription of the *Per1* and *Per2* circadian clock genes indicating that CRY1 and CRY2 function as negative regulators of these genes (30). Indeed, transient transfection/reporter gene assays have shown that both CRY1 and CRY2 bind to the clock proteins BMal1 and CLOCK that are positive transcription factors and suppress their transcription-stimulating activities (21). Interestingly, CRY2, in addition to its transcription inhibitory function, also acts as a transcriptional stimulator of *BMal1* gene by an unknown mechanism (35). In light of these previous data on light-independent gene regulatory functions of CRYs, our finding that CRY2 is a DNA binding protein may be relevant to its dark rather than light function.

It is conceivable that some of the transcription regulatory activities of CRYs are mediated by direct CRY–DNA interaction rather than through the intermediacy of other clock proteins. Along these lines, we tested the E-box element, which is found in the promoter of several clock genes for specific binding to hCRY2 but did not detect preferential binding to this sequence (data not shown). It is possible some other clock gene-specific sequences are high affinity binding sites for CRY. Further work is required to address this possibility. Previous attempts to investigate CRY–DNA interactions have resulted in conflicting data. In one study, it was simply reported that neither recombinant hCRY1 and hCRY2 made in *E. coli* nor the proteins existing in HeLa cells constitutively had DNA repair activity (11). DNA binding was not addressed in that study. In another study, recombinant hCRY1 was tested for DNA binding, and it was found to lack DNA binding activity either with undamaged or UV-irradiated DNA (36). In a third study, it was reported that mouse CRY1 (which is 95% identical to human CRY1) bound to a DNA cellulose column but that mouse CRY2 (95% sequence identity to human CRY2) did not bind to the column (37). In this latter study, the CRY proteins–DNA cellulose interaction was probed by immunoblotting of cell extracts applied to column and eluted with a salt gradient. We do not have a satisfactory explanation for the conflicting results regarding CRY1 binding to DNA and the failure to detect binding of CRY2 to DNA. It must be noted, however, that in this study in contrast to all earlier work (11, 36, 37) we use CRY purified from its native source, and all of the experiments were performed with protein purified to near-homogeneity. Therefore, we believe that the current results represent an intrinsic property of cryptochromes. Indeed, we have found similar DNA binding with hCRY1 (data not shown). Finally, the relatively specific binding of hCRY2 to the (6-4) photoproduct deserves some comment. It could be an evolutionary relic reflecting a common origin with photolyases. It is also possible that the structural change caused by the (6-4) photoproduct is similar to a particular DNA structure associated with a transcription regulatory element as has been found for certain transcription factors that bind with relatively high specificity to damaged DNA (38, 39).

ACKNOWLEDGMENT

We thank Dr. Brenda Temple for helping with the molecular modeling of hCRY2, Drs. Ryujiro Hara and Joyce Reardon for the oligomer containing the (6-4) photoproduct, and Dr. Halil Kavakli for the critical reading of the manuscript.

REFERENCES

1. Sancar, A. (2000) *Annu. Rev. Biochem.* 69, 31–67.
2. Lin, C. (2002) *Plant Cell* 14, 5207–5215.
3. Van Gelder, R. N. (2002) *J. Biol. Rhythms* 17, 110–120.
4. Ahmad, M. (1999) *Curr. Opin. Plant Biol.* 2, 230–235.
5. Hall, J. C. (2000) *Curr. Opin. Neurobiol.* 10, 456–466.
6. Sancar, A. (1994) *Biochemistry* 33, 2–9.
7. Todo, T. (1999) *Mutat. Res.* 434, 89–97.
8. Deisnehofer, J. (2000) *Mutation Res.* 460, 143–149.
9. Malhorta, K., Kim, S. T., Batschauer, A., Dawut, L., and Sancar, A. (1995) *Biochemistry* 34, 6892–6899.
10. Lin, C., Robertson, D. E., Ahmad, M., Raibekas, A. A., Jorns, M. S., Dutton, P. L., and Cashmore, A. R. (1995) *Science* 269, 968–970.
11. Hsu, D. S., Zhao, X., Zhao, S., Kazantsev, A., Wang, R. P., Todo, T., Wei, R. F., and Sancar, A. (1996) *Biochemistry* 35, 13871–13877.
12. Ahmad, M., Grancher, N., Heil, M., Black, R. C., Giovani, B., Galland, P., and Lardemer, D. (2002) *Plant Physiol.* 129, 774–785.
13. Miyamoto, Y., and Sancar, A. (1998) *Proc. Natl. Acad. Sci. U.S.A.* 95, 6097–6102.
14. Miyamoto, Y., and Sancar, A. (1999) *Mol. Brain Res.* 71, 248–253.
15. Park, H. W., Kim, S. T., Sancar, A., and Deisnehofer, J. (1995) *Science* 268, 1866–1872.
16. Tamada, T., Kitadokora, K., Higuchi, Y., Inaka, K., Yasui, A., deRuiter, P. E., Eker, A. P. M., and Miki, K. (1997) *Nat. Struct. Biol.* 11, 887–891.
17. Zhao, X., Liu, J., Hsu, D. S., Zhao, S., Taylor, J. S., and Sancar, A. (1997) *J. Biol. Chem.* 272, 32580–32590.
18. Husain, I., and Sancar, A. (1987) *Nucleic Acids Res.* 15, 1109–1120.
19. Kiener, A., Husain, I., Sancar, A., and Walsh, C. (1989) *J. Biol. Chem.* 264, 13880–13887.
20. Thresher, R. J., Vitaterna, M. H., Miyamoto, Y., Kazantsev, A., Hsu, D. S., Petit, C., Selby, C. P., Dawut, L., Smithies, O., Takahashi, J. S., and Sancar, A. (1998) *Science* 282, 1490–1494.
21. Kume, K., Zylka, M. J., Sriram, S., Shearman, L. P., Weaver, D. R., Jin, X., Maywood, E. S., Hastings, M. H., and Reppert, S. M. (1999) *Cell* 98, 193–205.
22. Ceriani, M. F., Darlington, T. K., Staknis, D., Mas, P., Petti, A. A., Weitz, C. J., and Kay, S. A. (1999) *Science* 285, 553–556.
23. Johnson, J. L., Hamm-Alvarez, S., Payne, G., Sancar, G. B., Rajagopalan, K. V., and Sancar, A. (1988) *Proc. Natl. Acad. Sci. U.S.A.* 85, 2046–2050.
24. Jorns, M. S., Sancar, G. B., and Sancar, A. (1984) *Biochemistry* 23, 2673–2679.
25. Cashmore, A. R., Jarillo, J. A., Wu, Y. J., and Liu, D. (1999) *Science* 284, 760–765.
26. Todo, T., Ryo, H., Yamamoto, K., Toh, H., Inui, T., Ayaki, H., Nomura, T., and Ikenaga, M. (1996) *Science* 272, 109–112.
27. Ahmad, M., and Cashmore, A. R. (1993) *Nature* 366, 162–166.
28. Lin, C., Ahmad, M., and Cashmore, A. R. (1996) *Plant J.* 10, 893–902.
29. Stanewsky, R., Kaneko, M., Emery, P., Berets, B., Wager-Smith, K., Kay, S. A., Rosbash, M., and Hall, J. C. (1998) *Cell* 95, 681–692.
30. Vitaterna, M. H., Selby, C. P., Todo, T., Niwa, H., Thompson, C., Fruechte, E. M., Hitomi, K., Thresher, R. J., Ishikawa, T., Miyazaki, J., Takahashi, J. S., and Sancar, A. (1999) *Proc. Natl. Acad. Sci. U.S.A.* 96, 12114–12119.
31. Selby, C. P., Thompson, C., Schmitz, T. M., Van Gelder, R. N., and Sancar, A. (2000) *Proc. Natl. Acad. Sci. U.S.A.* 97, 14697–14702.
32. Van Gelder, R. N., Wee, R., Lee, J. A., and Tu, D. C. (2003) *Science* 299, 222.
33. Shalitin, D., Yang, H., Mockler, T. C., Maymon, M., Gud, H., Whitlam, G. C., and Lin, C. (2002) *Nature* 417, 763–767.
34. Rosato, E., Codd, V., Mazzotta, G., Piccin, A., Zordan, M., Costa, R., and Kyriacou, C. P. (2001) *Curr. Biol.* 11, 909–917.
35. Reppert, S. M., and Weaver, D. R. (2002) *Nature* 418, 935–941.
36. Todo, T., Tsuji, H., Otsu, E., Hitomi, K., Kim, S. T., and Ikenaga, M. (1997) *Mutat. Res.* 384, 195–204.
37. Kobayashi, K., Kanno, S., Smit, B., van der Horst, G. T. J., Takao, M., and Yasui, A. (1998) *Nucleic Acids Res.* 22, 5086–5092.
38. Pil, P. M., and Lippard, S. J. (1992) *Science* 256, 234–237.
39. Treiber, D. K., Zhai, X., Jantzen, H. M., and Essigmann, J. M. (1994) *Proc. Natl. Acad. Sci. U.S.A.* 91, 5672–5676.

BI026963N